Available online at www.sciencedirect.com

SciVerse ScienceDirect

Journal of the European Ceramic Society 32 (2012) 3043–3049

www.elsevier.com/locate/jeurceramsoc

Fabrication and microstructure investigation of ultra-high-strength porcelain insulator

Yong Meng [a,b], Guohong Gong [b,*], Zhengping Wu [c], Zhongju Yin [c], Yumin Xie [c], Shirong Liu [b]

[a] *Graduate School of Chinese Academy of Sciences, Beijing 100049, China*
[b] *State Key Laboratory of Ore Deposit Geochemistry, Institute of Geochemistry, Chinese Academy of Sciences, Guiyang 550002, Guizhou, China*
[c] *Bijie Highland Porcelain Insulator Limited Liability Company, Bijie 551700, Guizhou, China*

Received 17 February 2012; received in revised form 6 April 2012; accepted 10 April 2012
Available online 9 May 2012

Abstract

Insulators are essential components of power transmission network. With natural minerals such as bauxite and clay, we have fabricated ultra-high-strength porcelain insulator (UHSPI) of electromechanical failure load 420 kN determined by International Electrotechnical Commission (IEC), and have put it into production. Compared with other UHSPI fabricating methods, in which industrial alumina is used, our method is cost saving and rich in resources. The main objective of the study is to elucidate the relationship between microstructure (e.g. size, amounts and distribution of particles) and mechanical property of the sintered UHSPI and thereby to explore a way to further improve the mechanical property of UHSPI. The investigations of SEM, EDAX and XRD reveal that the strengthening mechanisms may be the combination of matrix reinforcement, mullite reinforcement and dispersion strengthening; high porosity (9.9%) and abnormal pores are more possible to be the main factor hindering electromechanical property improvement.

Keywords: Insulator; Microstructure; Properties; Minerals; Strengthening mechanism

1. Introduction

Insulators are essential components widely used on power transmission network. As such, the properties of eligible insulators are high mechanical strength, high resistivity, corrosion resistance, etc.[1,2] Before put into application, insulators must pass the IEC specified 20 standard property tests (e.g. electromechanical failure load test, flash test, power frequency sparking test, more details in IEC 60383-1:1993 MOD standard), which are generally accepted in the field of insulator. The tests involve many aspects of insulator such as electromechanical properties and external dimension. What's more, the tests are strict to guarantee safety, and this is also the reason why it is difficult to get the qualification certificate issued by IEC.

Porcelain insulators have been used more than 160 years.[1,3,4] During the period, three kinds of porcelain insulators had appeared in the order of feldspar insulator, cristobalite insulator and alumina insulator.[5] Alumina insulator belongs to UHSPIs and is widely used in power transmission network due to its advantages such as excellent mechanical properties and distinguished corrosion resistance. The electromechanical failure load is one of the most important properties of insulator. The uppermost electromechanical failure load enacted by IEC is 530 kN. To the best of our knowledge, there is rarely a manufacturer reaching this level, but we are on the way to this goal. Up to now, we have successfully fabricated UHSPI of electromechanical failure load 420 kN determined by IEC with natural minerals such as bauxite and clay, and have put it into production. Compared with other UHSPI fabricating methods in which industrial alumina is used (e.g. UHSPI of the famous NGK Corporation whose raw materials contains 20 wt% industrial alumina), our method of UHSPI fabricating is cost saving and rich in resources.

As regards the mechanisms on enhancing the mechanical properties of porcelain insulators, three mechanisms (i.e. mullite strengthening theory, dispersion strengthening theory and matrix reinforcement theory) had been presented.[6,7] The mullite strengthening theory maintains that the strength of porcelain insulator solely lies on the amount and size of mullite needles

* Corresponding author. Tel.: +86 0851 5891606; fax: +86 0851 5891606.
E-mail address: gongguohong@vip.gyig.ac.cn (G. Gong).

0955-2219/$ – see front matter © 2012 Elsevier Ltd. All rights reserved.
http://dx.doi.org/10.1016/j.jeurceramsoc.2012.04.015

which act as interlocks in the matrix; the dispersion strengthening theory suggests that strength enhancing results from microcrack propagating hindered by particles such as corundum that dispersed in the vitreous phase of a porcelain insulator body; the matrix reinforcement theory argues that mechanical property benefits from compressive stresses indwelling in the vitreous phase caused by difference in thermal expansion coefficients between crystalline phases or particles and the surrounding vitreous phase. In addition, the glaze on the surface of UHSPI is also of great effect on the mechanical strength of UHSPI, which is confirmed in the study. The most popular approach used to improve the mechanical property of UHSPI is to enhance the amount of crystal phases such as mullite and corundum. Moreover, decreasing the sizes of both particles and pores also contributes to the mechanical property of UHSPI.

In present work, an attempt is made to elucidate the relationship between microstructure (e.g. size, amounts and distribution of particles) and mechanical property of the sintered UHSPI and thereby to explore a way to further improve the mechanical property of UHSPI.

2. Experimental procedure

2.1. Fabrication

The starting materials used for the green body of the sample were: 40 wt% bauxite (calcined at 1500 °C before mixing for the purpose of getting more corundum), 35 wt% Qiantao clay, 10 wt% Xiaohe clay, 15 wt% feldspar, while that of the glaze were: 26 wt% feldspar, 10 wt% Qiantao clay, 11 wt% talc, 33 wt% quartz, 12 wt% Xiaohe clay, 7 wt% calcite. The raw materials used were offered by our mines except quartz. Before applying, they should be conducted with a few analyses such as XRD, XRF for determining the contents of useful or detrimental components such as Fe_2O_3 and TiO_2. The composition purity requirements for raw materials are presented in Table 1.

The bauxite used was processed in the industrial flow of mining, separating from impurities, crushing into small pieces <50 mm, pressing into compacts, calcining at 1500 °C for 24 h in rotary kiln, crushing, micronizing. The bauxite used mainly composed of diaspore ($Al_2O_3{\cdot}H_2O$) with small amount of kaolinite ($Al_2O_3{\cdot}2SiO_2{\cdot}2H_2O$), pyrophyllite ($Al_2O_3{\cdot}4SiO_2{\cdot}H_2O$), etc. The heating process up to 1500 °C could be divided into two stages.[8,9] The first stage ($T < 900$ °C) is dehydration, including diaspore dehydration (400–580 °C), kaolinite dehydration (400–700 °C) and pyrophyllite dehydration (700–900 °C), etc. During this stage, α-Al_2O_3 is produced directly by dehydration of diaspore, and is of high specific surface area and lower crystallinity.[10] In the second stage (900–1500 °C), the α-Al_2O_3 will become denser with the increasing of calcination temperature. The α-Al_2O_3 particle resulting from diaspore is usually characterized by a few pinholes in itself.

The chemical compositions for green body and glaze are presented in Table 2. The sample was fabricated at the Bijie Highland Porcelain Insulator Limited Liability Company, in the industrial flow of raw materials mixing, ball milling, stirring, sieving, deironing, pug milling, staling, shaping, drying, glazing, sintering. Particles size distribution for ball milled mixtures was: ≥5 μm accounting for 45–50%, ≥10 μm accounting for 25–30%, ≥20 μm accounting for 5–10%, ≥50 μm accounting for 0%. The glazed green body was sintered in drawer-like kilns under the control of computer with given procedures. The average heating rate was 9.1 °C/h up to the upmost sintering temperature 1270 °C, and then the sample was furnace cooled to ambient temperature with an average rate of 19.2 °C/h. In particular, the cooling rate at the temperature of β–α transformation of quartz (around 573 °C) should be low. To summarize, the average variation rate of temperature was low for the purpose of making the sample sintered completely.

The heating process above could be classified into two major stages by resultant state. The first stage ($T < 980$ °C) is mainly gas exhaust, namely, the decomposition of hydrate, organics, sulfide and carbonate, etc.[8] During this period, a great deal of heat is required. The heating rate should be moderate as much as possible, otherwise the deformation of the samples would be serious. The second stage (980–1300 °C) is mainly the stage of mullitization and densification. Based on the previous literatures[8,11,12] and mineral compositions of our porcelain, the potential phase evolutions of the body on the second stage were summarized as follows:

When $T \sim 980$ °C, $3(Al_2O_3{\cdot}2SiO_2)$ (metakaolinite) $\rightarrow 3Al_2O_3{\cdot}2SiO_2$ (primary mullite) + $4SiO_2$ (amorphous) (1); or $Al_2O_3{\cdot}2SiO_2$ (metakaolinite) $\rightarrow 2Al_2O_3{\cdot}3SiO_2$ (spinel) + SiO_2 (amorphous) (2); or $Al_2O_3{\cdot}2SiO_2$ (metakaolinite) $\rightarrow Al_2O_3$ (γ-alumina) + $2SiO_2$ (amorphous) (3).

When $T > 1100$ °C, $3(Al_2O_3{\cdot}4SiO_2)$ (pyrophyllite relict) $\rightarrow 3Al_2O_3{\cdot}2SiO_2$ (primary mullite) + $10SiO_2$ (amorphous) (4); $3(2Al_2O_3{\cdot}3SiO_2)$ (spinel) $\rightarrow 2(3Al_2O_3{\cdot}2SiO_2)$ (primary mullite) + $5SiO_2$ (amorphous) (5).

When $T > 1150$ °C, $K_2O{\cdot}Al_2O_3{\cdot}6SiO_2$ (orthoclase) $\rightarrow K_2O{\cdot}Al_2O_3{\cdot}4SiO_2$ (leucite) + $2SiO_2$ (glass) (6); Al_2O_3 (γ-alumina) + $2SiO_2$ (amorphous) $\rightarrow 2(3Al_2O_3{\cdot}2SiO_2)$ (secondary mullite) (7); SiO_2 (amorphous) $\rightarrow SiO_2$ (cristobalite) (8). The existence of feldspars could lower melt temperature and viscosity of liquid phase, which in turn contributes to the nucleation and growth of secondary mullite crystals and thus increases the final density of porcelain body.

2.2. Characterization

2.2.1. SEM, EDAX and XRD analyses

The microstructure of the sample was investigated by Scanning Electron Microscopy (model: JSM-6490LV, Japan) on samples polished, etched with a solution containing 20 vol% HF for 30 s and coated with a carbon layer, combined with Energy Disperse Spectroscopy (model: EPMA-1600, Shimadazu Ltd., Japan) for chemical analysis. Crystal phases identification for the body of sample was performed by X-ray diffraction with a diffractometer (model: D/Max2200, Japan) using nickel filtered Cu Kα radiation ($\lambda = 1.54178$ Å). Working voltage and current were 40 kV and 30 mA, respectively. The pattern were recorded in the 2θ range of 3–60 °, in the mode of step-scanning with 0.04° in step size and a counting time of 5 s per step. The crystalline phases in the resulting sample were determined by

Table 1
Composition purity requirements for raw materials (wt%).

	Bauxite	Quartz	Clays	Feldspar	Calcite	Talc
Requirements	Al_2O_3 >85%	SiO_2 >99%	(Fe_2O_3, TiO_2) <3.5%	Fe_2O_3 <1%; (Ka_2O, Na_2O) >12%	Fe_2O_3 <1%; CaO >54%	Fe_2O_3 <1%; MgO >30%

Table 2
Ratio (wt%) of chemical compositions for green body and glaze of the sample determined by XRF.

	Al_2O_3	SiO_2	K_2O	TiO_2	Fe_2O_3	Na_2O	CaO	MgO	Ablation ratio
Green body	45.30	45.10	2.85	1.75	0.81	0.74	0.43	0.35	3.5
Glaze	14.40	68.60	3.12	0	0.41	0.75	4.11	3.15	4.90

comparing their XRD patterns with the standard patterns of various crystalline phases which were possible to form in the sample under the given conditions. The phase identification and content calculation were carried out with software JADE 5.

2.2.2. Bending strength test

For the purpose of investigating the effect of glaze on the bending strength of sample, two groups of bars (one group was of a glaze 0.3 mm in thickness, while the other was not; each group including 15 one) of ∅1.5 cm × 10.7 cm (length) were prepared for bending strength test on a universal materials tester (model: W-60, Jinan, China). The starting materials and processing of the bars were same with the sample.

2.2.3. IEC tests

80 samples were sent to CHINA NATIONAL CENTER FOR QUALITY SUPERVISION AND TEST OF INSULATORS AND SURGE ARRESTERS (one of the actuators of IEC) for the IEC specified standard 20 property tests. All the samples passed the tests and got the qualification certificate (Grant No. WJ-301-2008). Electromechanical failure load is one of most important properties of insulator. Hence, the electromechanical failure load is taken as the grading standard of insulator. The electromechanical failure load test was performing on the sample with a tensile tester accompanying a 40 kV Power Frequency Voltage until destroyed. 10 samples were tested.

3. Results and discussion

3.1. XRD analysis

XRD pattern for the body of the sample is displayed in Fig. 1. The phase identification and content calculation were carried out with the software JADE 5. The content of the amorphous phase in the sample is calculated in the order of smoothing, background correction, amorphous peak fitting, crystal peak fitting, calculating (ratio of hump area to total area). The content of amorphous phase within the sample worked out to be 70 wt%. That is to say, the total content of crystalline phases is 30 wt%.

The content of each crystalline phase in the body of the sample was determined by *K*-value method in which *K*-value (i.e. RIR) could be gotten from PDF card or experiment. With

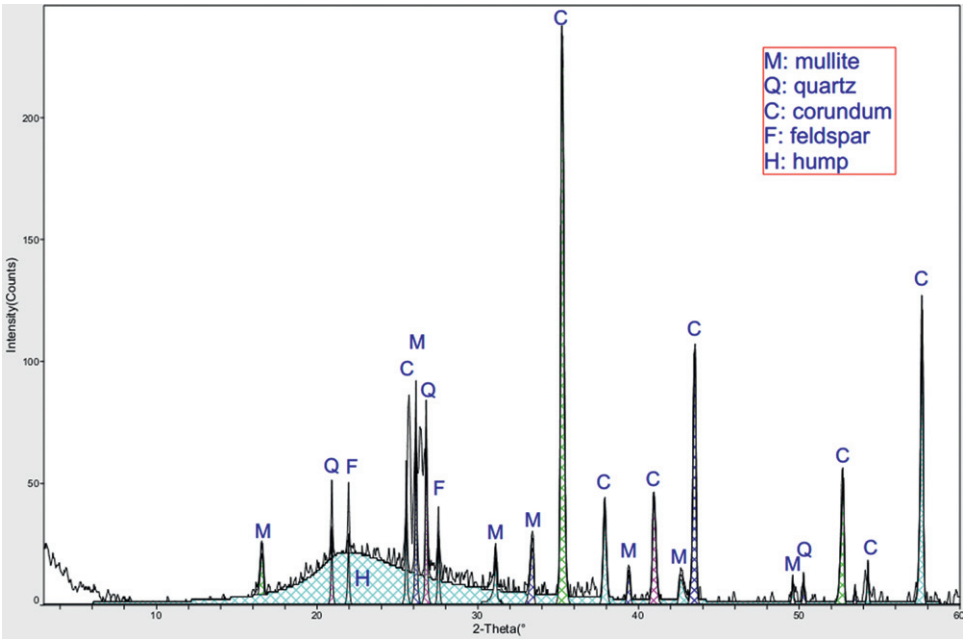

Fig. 1. XRD pattern (processed by JADE 5) for the body of the sample.

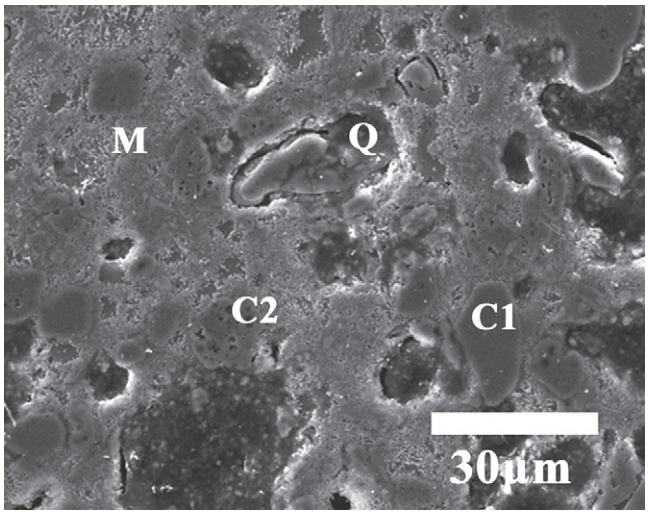

Fig. 2. SEM micrograph of the etched sample polished with a polishing paper accompanying with diamond paste (2.5 μm). Q, quartz; C1, corundum (α-alumina); C2, pinhole alumina; M, mullite.

K-value and intensity of characteristic peak of each crystalline phase, we could get the percentage of each crystalline phase to total amount of the crystalline phases. Finally, the content of each crystalline phase was worked out: 12 wt% corundum, 11 wt% mullite, 4 wt% quartz and 2 wt% feldspar.

3.2. Determination of grain class by EDAX and effects of grains on property

The composition of different spots in Fig. 2 (i.e. Q; C1; C2; M) is presented in Table 3 by EDXA. From the results it is obvious that Q is quartz; C1 is corundum; C2 with pinholes in itself may be γ-alumina, so-called active alumina, having a huge specific area larger than 200 m^2/g. There only exist small amounts of γ-alumina according to quantitative analysis results. So most of the pinhole alumina was α-alumina resulted from calcined bauxite, which is usually characterized by a few pinholes in itself. The pinhole of alumina could absorb gases in itself before sintering. Later when increasing temperature, gases in the pinhole may diffuse and expand, which facilitates pores formation. So the pinhole is detrimental in this sense. This is one imperfection of this fabricating method needing improvement.

The quartz particle always has a melted rim around itself for the reason that when above 1200 °C, quartz starts to melts, and a glass rim emerges. During the cooling, there is a significant β–α transformation of quartz at 573 °C resulting in a 2% decrease of the volume of quartz particle.[13] This will give rise to a compressive stress to the matrix, which is beneficial to improve bending strength according to the matrix reinforcement mechanism. It was also observed that quartz particles with a size larger than 30 μm always have circumferential crack, which is detrimental. It was reported that the optimum size range for quartz particles is 5–20 μm,[7] so further improving mechanical strength should pay close attention to factors related to size distribution of quartz particles.

Table 3
Composition of different spots (at%) determined by EDXA.

	Q	C1	C2	M
Al_2O_3	0	100	100	48.35
SiO_2	100	0	0	45.60
K_2O	0	0	0	00.87
TiO_2	0	0	0	03.13
FeO	0	0	0	02.05

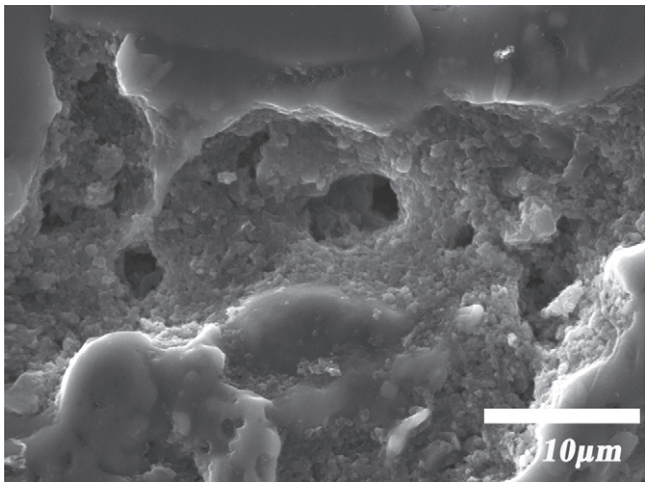

Fig. 3. SEM micrograph of abnormal pore in the sample.

Alumina and quartz particles are almost uniformly distributed in the matrix with a size range of <25 μm, while there occasionally exist some abnormal particles which are large, irregular, and even having a few aggregations of pinhole alumina particles which are detrimental to the bending strength of sample. The presence of the particles such as corundum embedded in the glassy matrix, serve as hard barrier and thereby cause the deflection of crack when loading. As a result, more energy is needed for cracking. This is one of the reasons behind high strength, namely dispersion strengthening mechanism.[14]

3.3. Morphology, distribution and amount of pores

Most pores are spherical or elliptic, and homogeneously distributed in the matrix, while a few pores are elongated or interconnected. The size of most pores is in the range of 1–25 μm. It was reported[7,15,16] that spherical, uniformly distributed pores less than 20 μm have a positive effect on the bending strength of porcelains, which may be one of the reasons behind high strength. But there still occasionally exist some abnormal pores (Fig. 3) which are large or irregular or interconnected. Those abnormal pores are detrimental to the mechanical property of the sample because they may serve as the origin of fracture. Pores are inevitable because of the decomposition of organic and inorganic compounds in the green body, or for other reasons.

Based on the observation that pores were homogeneously distributed in the matrix, the total porosity (9.9%) was calculated by the area percentage of pores. The existence of pores in the matrix immediately hinders body densification resulting in the decrease of effective loading area and dielectrical property. Crack is rare in the body of the sample, while the body is

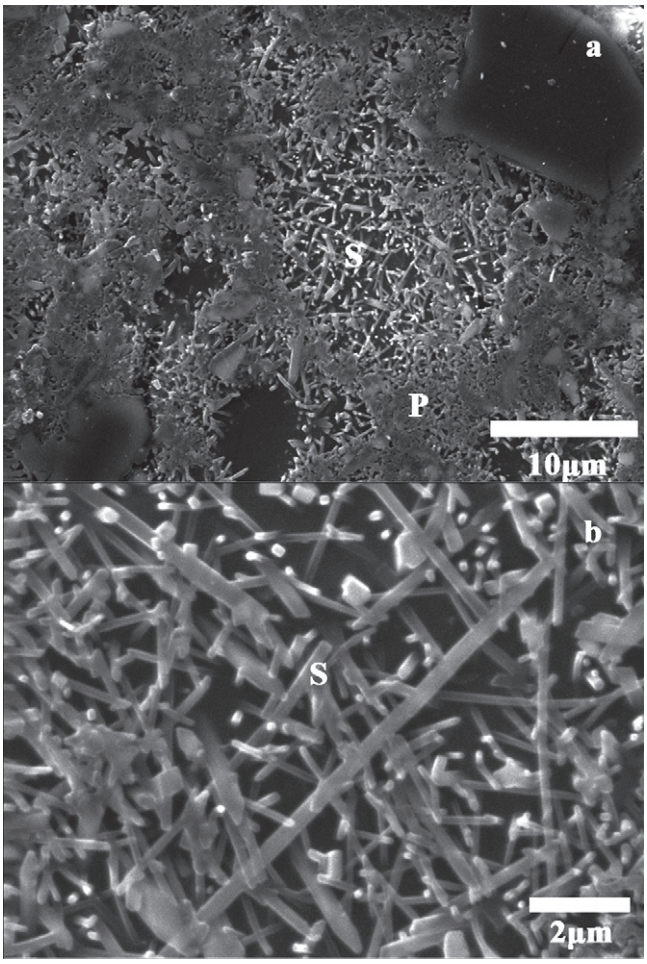

Fig. 4. SEM micrograph of the etched sample about mullite. S, secondary mullite; P, primary mullite.

of a high porosity (9.9%) and abnormal pores which are large or elongated or interconnected. So pores may be the main factor hindering electromechanical properties improvement.[15,16] To improve the properties of the sample, one should decrease the porosity as much as possible. It was reported[17] that finer milled raw materials with a narrow size distribution could both reduce the amount and size of pores. So milling processes should be taken into account for further improvement of electromechanical properties.

3.4. Class, morphology and effect of mullite

Two kinds of mullite were observed (Fig. 4) in the body of the sintered UHSPI, namely primary mullite and secondary mullite. The primary mullite resulted from transformation of metakaolin, pyrophyllite, etc., is dense and short, while the secondary mullite produced by reaction between clay and feldspar relicts at ~1200 °C[18,19,20] is needle-like and interlocking with a size range of 1–15 μm in length. The interlocked structure of mullite with acicular morphology favors the promotion of mechanical properties according to the mullite strengthening theory. What's more, the formation of mullite from clay matrix will increase volume by 10% (compared to precursor of mullite).[21] The increase

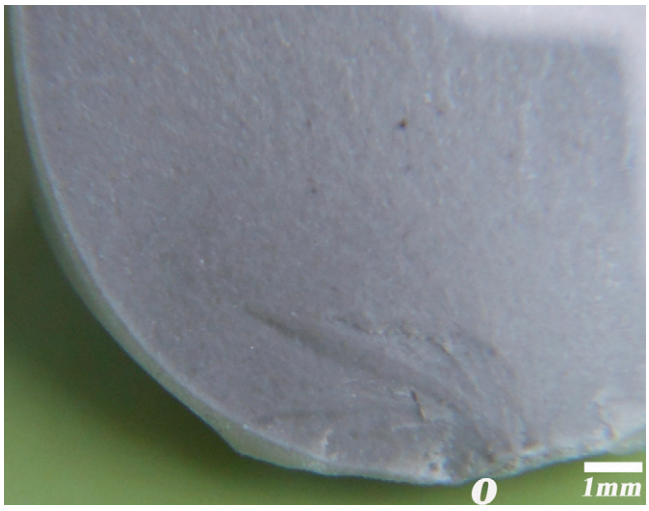

Fig. 5. Representative optical micrograph of fracture surface of the bars. O, origin of the fracture.

in volume could heal up cavity or porosity or crack formed due to shrinkage or other reasons. It is observed that in areas where mullite is abundant, the size and amounts of pores or cracks are small, which is in accordance with the mullite strengthening theory. The stoichiometric formula of mullite is $3Al_2O_3{\cdot}2SiO_2$ where the ratio of aluminum to silicon is 3:1, while the ratio of aluminum to silicon of raw materials is 0.6:1 (smaller than 3:1). This may be one of the reasons why the content of mullite (11 wt%) is relatively low. Further improving the content of mullite is a significant way to enhance the mechanical properties of UHSPI.

3.5. Effect of glaze on bending strength of bars

The bending strength of glazed and unglazed bars is shown in Table 4. The average bending strength of glazed and unglazed bars is 186 MPa with a standard deviation (11.2 MPa) and 143 MPa with a standard deviation (11.6 MPa), respectively. Compared with bending strength reported by Chan et al. (75.7 MPa)[21] and Alarcón et al. (125 MPa),[18] it has been greatly improved; compared to the unglazed bars, the bending strength of the glazed bars is improved by 30%. It was observed that the fracture of the bending bars always started from area near the surface (e.g. Fig. 5). The reason behind this may be that area near surface suffered a bigger stress than other area did when loading. There is rarely a crack observed in the body, while there is a high porosity (9.9%) and abnormal pores which are large or elongated or interconnected in the body. Large pores near the surface area are therefore more possible to serve as the origin of fracture.[15] The glaze could effectively fill the pores on the surface and retard cracking, Thereby promoting the bending strength of the bars.

3.6. Electromechanical failure load

The results of the electromechanical failure load test are shown in Table 5. The average electromechanical failure load

Table 4
Bending strength of glazed and unglazed bars (MPa).

	1	2	3	4	5	6	7	8	9	10	11	12	13	14	15
Glazed	181	165	190	180	193	196	198	182	167	205	186	178	187	198	184
Unglazed	135	150	142	131	132	162	127	134	126	145	149	147	156	152	157

Table 5
Electromechanical failure load (E) determined by IEC.

	1	2	3	4	5	6	7	8	9	10
E (kN)	479	510	496	518	481	468	529	539	527	514

Table 6
Differences between our porcelain and porcelain of Chan et al. [21].

	Our porcelain	Porcelain of Chan et al.
Main compositions	45.30 wt% Al_2O_3, 45.10 wt%SiO_2	22.64 wt% Al_2O_3, 70.03 wt%SiO_2
Bauxite (calcined)	40 wt% bauxite was added in	Without bauxite/industrial alumina
Max sintering temperature	1270 °C	1350 °C
Crack	Rare	Very common
Porosity	About 9.9%	Small
Major particle	Corundum	Quartz
Secondary mullite	Rich	Rare
Mean bending strength	143 MPa (unglazed)	75.7 MPa
Major defect	High porosity and abnormal pore	Mass crack and high SiO_2 content

($\bar{E}$) is 506 kN with a standard deviation (σ) value (24 kN). The safety level determined by IEC is 420 kN. $\bar{E} - 3^*\sigma = 434\,\text{kN} >$ 420 kN. Still there is many other IEC tests information about this sample. Due to the length limitation, we just present this one here.

3.7. Comparisons with work of peers

The research on porcelain insulator has continued more than 160 years since 1850 when insulator was introduced in the construction of power transmission network by Werner Von Siemens.[2] A series of fabrication methods were developed by companies and institutes. It could be helpful to make comparisons with previous work of peers for further improvement of fabrication method. The differences between our porcelain and porcelain of Chan et al.[21] are presented in Table 6.

4. Conclusions

The sample of electromechanical failure load 420 kN was fabricated successfully with natural minerals such as bauxite and clay. Compared with other UHSPI fabricating methods, in which industrial alumina is used, our UHSPI fabricating method is cost saving and rich in resources. Most particles such as alumina and quartz with a size range of <25 μm, which are almost uniformly distributed in the matrix, serve as hard obstacles hindering the propagation of cracks when loading. Most pores with a size range of <25 μm are spherical or elliptic and homogeneously distributed in the matrix. Mullite with a size range of <15 μm is needle-like acting as interlocks. Abnormal pores and high porosity (9.9%) are more possible to be the main factor hindering electromechanical properties improvement. The glaze could effectively fill the pores on the surface and retard cracking, Thereby promoting the bending strength of the bars. The strengthening mechanisms of the sample may be the combination of matrix reinforcement, mullite reinforcement and dispersion strengthening.

Acknowledgments

This work is supported by the National Science and Technology Supporting Plan (Grant No. 2009BAF43B00), Academy-Region Cooperation Project of Chinese Academy of Sciences (Grant No. 2009-5-27).

Appendix A. Supplementary data

Supplementary data associated with this article can be found, in the online version, at http://dx.doi.org/10.1016/j.jeurceramsoc.2012.04.015.

References

1. Amigó JM, Serrano FJ, Kojdecki MA, Bastida J, Esteve V, Reventós MM, et al. X-ray diffraction microstructure analysis of mullite, quartz and corundum in porcelain insulators. *J Eur Ceram Soc* 2005;**9**:1479–86.
2. Amigó JM, Clausell JV, Esteve V, Delgado JM, Reventós MM, Ochando LE, et al. X-ray powder diffraction phase analysis and thermomechanical properties of silica and alumina porcelains. *J Eur Ceram Soc* 2004;**1**:75–81.
3. Liebermann J. The standard and trend for alumina porcelain insulators. *CFI – Ceram Forum Int* 2000;**6**:17–23.
4. Liebermann J. Reliability of materials for high-voltage insulators. *Am Ceram Soc Bull* 2000;**5**:55–8.

5. Liebermann J. Avoiding quartz in alumina porcelain for high-voltage insulators. *Am Ceram Soc Bull* 2001;**6**:37–41.
6. Carty WM, Senapati U. Porcelain-raw materials, processing, phase evolution, and mechanical behavior. *J Am Ceram Soc* 1998;**1**:3–20.
7. Stathis G. Effect of firing conditions, filler grain size and quartz content on bending strength and physical properties of sanitaryware porcelain. *J Eur Ceram Soc* 2004;**8**:2357–66.
8. Zhongzheng Y, Daoyuan Y, Shunbo Z, Zhenxian X, Zhanfang G. Phase transition of preparing mullite materials with bauxite in heating process. *Mater Rev* 2010:502–5 [in Chinese with English abstract].
9. Boumaza A, Djelloul A, Guerrab F. Specific signatures of α-alumina powders prepared by calcination of boehmite or gibbsite. *Powder Technol* 2010;**2**:177–80.
10. Tsuchida T. Preparation and reactivity of acicular α-Al_2O_3 from synthetic diaspore, β-$Al_2O_3 \cdot H_2O$. *Solid State Ionics* 1993;**0**:464–70.
11. Chen CY, Lan GS, Tuan WH. Microstructural evolution of mullite during the sintering of kaolin powder compacts. *Ceram Int* 2000;**7**:715–20.
12. Ribeiro MJ, Tulyagavov DU, Ferreira JM, Labrincha JA. High temperature mullite dissolution in ceramic bodies derived from Al-rich sludge. *J Eur Ceram Soc* 2005;**5**:703–10.
13. Chmelík F, Trník A, Stubna I, Pesicka J. Creation of microcracks in porcelain during firing. *J Eur Ceram Soc* 2011;**13**:2205–9.
14. Carbajal L, Rubiomarcos F, Bengochea M, Fernandez J. Properties related phase evolution in porcelain ceramics. *J Eur Ceram Soc* 2007;**13–15**:4065–9.
15. Liebermann J, Schulle W. Bauxite porcelain – a new high-tech product for high-voltage insulation. *Am Ceram Soc Bull* 2002;**2**:33–8.
16. Liebermann J, Schulle W. Bauxite porcelain: a new high-tech product for high-voltage insulation. *Am Ceram Soc Bull* 2002;**3**: 1727–30.
17. Amoros J, Orts M, Garciaten J, Gozalbo A, Sanchez E. Effect of the green porous texture on porcelain tile properties. *J Eur Ceram Soc* 2007;**5**:2295–301.
18. Montoya N, Serrano FJ, Reventós MM, Amigo JM, Alarcón J. Effect of TiO_2 on the mullite formation and mechanical properties of alumina porcelain. *J Eur Ceram Soc* 2010;**4**:839–46.
19. Lee WE, Souza GP, McConville CJ, Tarvornpanich T, Iqbal Y. Mullite formation in clays and clay-derived vitreous ceramics. *J Eur Ceram Soc* 2008;**2**:465–71.
20. Lee WE, Iqbal Y. Influence of mixing on mullite formation in porcelain. *J Eur Ceram Soc* 2001;**14**:2583–6.
21. Islam RA, Chan YC, Islam MF. Structure–property relationship in high-tension ceramic insulator fired at high temperature. *Mater Sci Eng B: Solid* 2004;**2**:132–40.